Citation: Molecular Therapy—Nucleic Acids (2015) 4, e247; doi:10.1038/mtna.2015.19

www.nature.com/mtna

Deep Sequence Analysis of AgoshRNA Processing Reveals 3' A Addition and Trimming

Alex Harwig[1], Elena Herrera-Carrillo[1], Aldo Jongejan[2], Antonius Hubertus van Kampen[2,3] and Ben Berkhout[1]

The RNA interference (RNAi) pathway, in which microprocessor and Dicer collaborate to process microRNAs (miRNA), was recently expanded by the description of alternative processing routes. In one of these noncanonical pathways, Dicer action is replaced by the Argonaute2 (Ago2) slicer function. It was recently shown that the stem-length of precursor-miRNA or short hairpin RNA (shRNA) molecules is a major determinant for Dicer versus Ago2 processing. Here we present the results of a deep sequence study on the processing of shRNAs with different stem length and a top G·U wobble base pair (bp). This analysis revealed some unexpected properties of these so-called AgoshRNA molecules that are processed by Ago2 instead of Dicer. First, we confirmed the gradual shift from Dicer to Ago2 processing upon shortening of the hairpin length. Second, hairpins with a stem larger than 19 base pair are inefficiently cleaved by Ago2 and we noticed a shift in the cleavage site. Third, the introduction of a top G·U bp in a regular shRNA can promote Ago2-cleavage, which coincides with a loss of Ago2-loading of the Dicer-cleaved 3' strand. Fourth, the Ago2-processed AgoshRNAs acquire a short 3' tail of 1–3 A-nucleotides (nt) and we present evidence that this product is subsequently trimmed by the poly(A)-specific ribonuclease (PARN).

Molecular Therapy—Nucleic Acids (2015) **4**, e247; doi:10.1038/mtna.2015.19; advance online publication 14 July 2015
Subject Category: siRNAs, shRNAs, and miRNAs

Introduction

The RNA interference (RNAi) mechanism uses small RNA molecules to control cellular gene expression.[1,2] These small molecules are processed from short RNA hairpin precursors of which the ends are defined by microprocessor cleavage (miRNAs)[3,4] or transcription initiation and termination (shRNAs).[5] In the canonical pathway, Dicer will cleave the top of the RNA hairpin to create a small RNA duplex with a 5' (5p) and 3' (3p) strand (**Figure 1a**; left panel).[6,7] Many of the Dicer-cleaved miRNA duplexes are subject to 3' end modification through addition of a few tailing nucleotides, specifically U or A.[8–10] The addition of 3' U is thought to mark the RNA for degradation[11–13] or processing.[14] Addition of 3'A is believed to promote stability,[15] but other reports failed to reproduce this effect.[8] The processed RNA duplex is loaded into the Argonaute (Ago)-containing RNA-induced silencing complex (RISC).[16–18] The PIWI domain of the Ago2 protein has slicing activity that cleaves the passenger strand, thus activating the guide strand.[19–21] The selection of guide/passenger is determined by the thermodynamic stability of the duplex ends.[22,23] The strand of which the 5' end is located at the least stable duplex end is more likely to be selected as guide. Guide-loaded RISC will target partially complementary messenger RNAs (mRNAs) for translational suppression or destruction.[18,24]

Recently, additional layers of complexity were added by the description of noncanonical RNAi pathways, specifically microprocessor-independent and Dicer-independent pathways.[25] In the latter, Ago2-slicer replaces Dicer for processing of certain miRNAs like miR-451 (refs. 26,27) and the subclass of shRNAs termed AgoshRNAs (**Figure 1a**; right panel). The short length of the miRNA/shRNA stem is a major determinant for entering this pathway.[28,29] A stem of 16–19 base pair (bp) is too small to serve as Dicer substrate and will consequently become an Ago2 substrate.[26,30–32] Ago2 cleaves halfway the 3' arm of the duplex between bp 10-11,[26,29] leaving a single guide strand of which the top remains base-paired (**Figure 1a**). MiR-451 is trimmed by PARN to create an unpaired guide (**Figure 1a**), but this modification has no significant effect on the silencing efficiency. It remains unclear if trimming also applies to the AgoshRNA class. It is important to learn such mechanistic details of AgoshRNA biogenesis as the property to generate a single guide strand could provide a major therapeutic benefit by avoiding passenger strand mediated off-target effects.[33]

In this manuscript, we present a deep sequencing study on the processing of shRNA and AgoshRNA variants. We selected the SOLiD method over 454/Illumina sequencing because the high yield of small RNAs and low error rate are perfectly suited for sequencing of miRNAs.[34] The hairpin variants that we analyzed were previously tested in luciferase knockdown experiments that suggested a shift from shRNA to AgoshRNA activity by stem shortening and a modulatory effect of a top G·U bp.[28] Northern blotting confirmed this shift by the appearance of the typical extended AgoshRNA guide molecule. We now present further details on Dicer-shRNA versus Ago2-AgoshRNA processing and 3' end modification.

[1]Laboratory of Experimental Virology, Department of Medical Microbiology, Center for Infection and Immunity Amsterdam (CINIMA), Academic Medical Center, University of Amsterdam, Amsterdam, The Netherlands; [2]Bioinformatics Laboratory, Department of Clinical Epidemiology, Biostatistics and Bioinformatics, Academic Medical Center, University of Amsterdam, Amsterdam, The Netherlands; [3]Biosystems Data Analysis, Swammerdam Institute for Life Sciences, University of Amsterdam, Amsterdam, The Netherlands Correspondence: Ben Berkhout, Laboratory of Experimental Virology, Department of Medical Microbiology, Center for Infection and Immunity Amsterdam (CINIMA), Academic Medical Center, University of Amsterdam, Meibergdreef 15, 1105 AZ, Amsterdam, The Netherlands. E-mail: b.berkhout@amc.uva.nl
Keywords: Ago2; AgoshRNAs; Dicer; deep sequencing; Dicer-independent shRNA; RNAi
Received 14 January 2015; accepted 6 May 2015; advance online publication 14 July 2015. doi:10.1038/mtna.2015.19

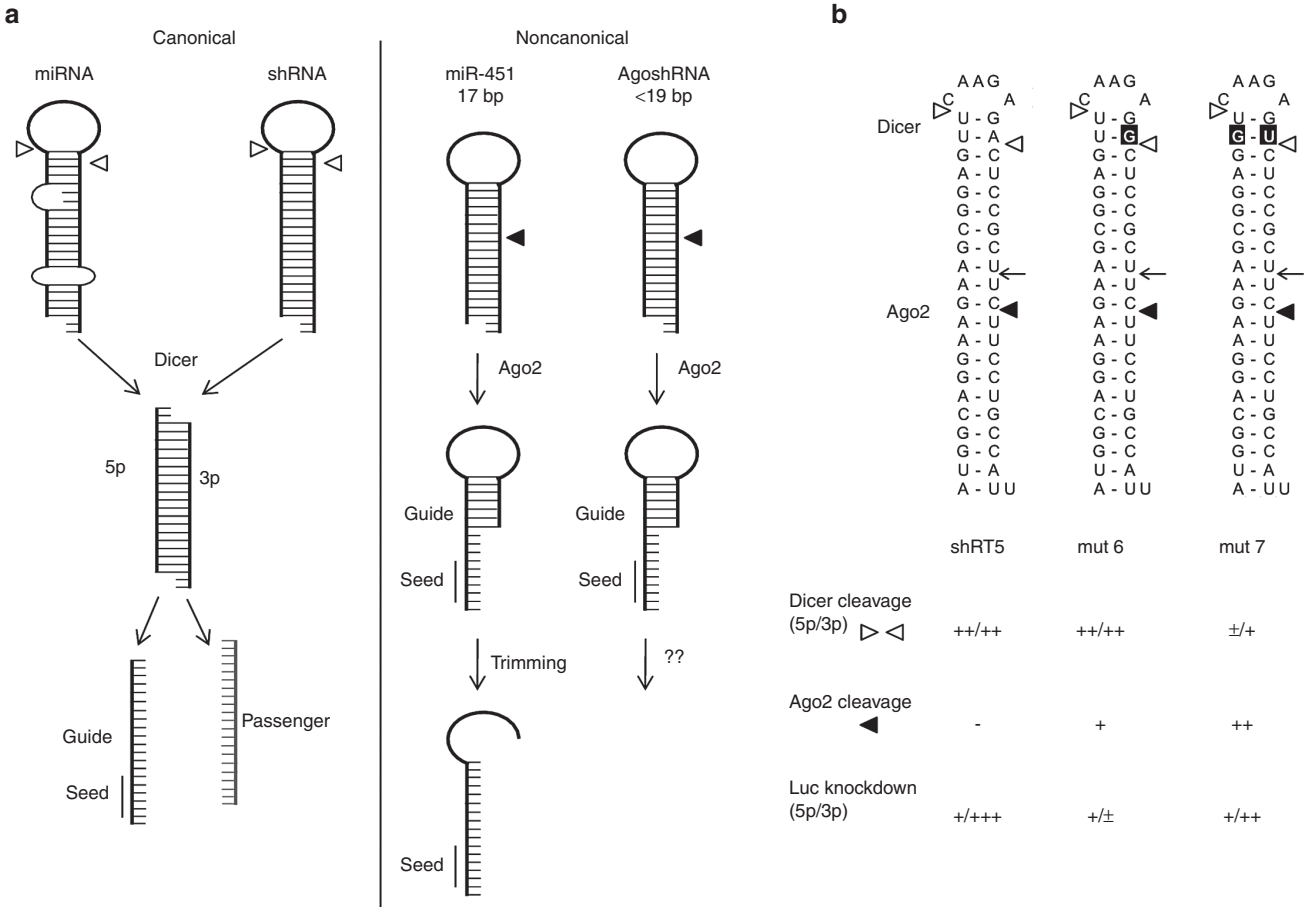

Figure 1 Canonical and noncanonical miRNA/shRNA processing. (**a**) Left panel: Dicer-dependent (canonical) processing is shown for miRNA and shRNA. Dicer cleavage (◅) yields 5' (5p) and 3' (3p) strands, the guide is loaded in RNA-induced silencing complex-Ago2 (black line with seed), the passenger is degraded (grey strand). Right panel: The Dicer-independent (non-canonical) miR-451 and AgoshRNA are processed by Ago2 (➡) to yield a single guide that is partially basepaired. Subsequent trimming of the 3' end opens miR-451. For AgoshRNAs, no such trimming has been described. (**b**) The wild-type shRT5 and two G-U mutants (mutations boxed in black) were studied by deep sequencing. Indicated are the predicted cleavage sites for Dicer and Ago2, but also the observed Ago2 cleavage site (←). Some key activities as measured previously are summarized below: Dicer and Ago2 products as scored on northern blot (see Figure 7 in reference [28]) and their activity on Luc-reporter assays (see Figure 6 Luc 5p: antisense; Luc 3p: sense in reference [28]).

Table 1 SOLiD deep sequence results

Name	Total	Unmapped	Mapped (%[a])	Mismatch (%[b])	No mismatch (%[b])	shRNA/ AgoshRNA (%[c])
shRT5	9,044,264	8,466,779	577,485 (6.4)	267,527 (46)	309,958 (54)	297,334 (96)
mut 6	7,455,000	7,213,851	241,149 (3.2)	117,354 (49)	123,795 (51)	122,742 (99)
mut 7	10,877,032	10,462,540	414,492 (3.8)	158,021 (38)	256,471 (62)	254,158 (99)
17GC	12,454,378	11,001,755	1,452,623 (11.7)	404,818 (28)	1,047,805 (72)	1,044,458 (100)
17GU	11,582,575	7,825,837	3,756,738 (32.4)	1,248,925 (33)	2,507,813 (67)	2,507,120 (100)
18GC	6,796,533	6,462,031	334,502 (4.9)	175,351 (52)	159,151 (48)	157,511 (99)
18GU	12,825,189	12,567,368	257,821 (2.0)	95,401 (37)	162,420 (63)	160,081 (99)
19GC	10,327,948	8,668,197	1,659,751 (16.1)	828,914 (50)	830,837 (50)	806,987 (97)
19GU	8,955,847	8,279,377	676,470 (7.6)	242,045 (36)	434,425 (64)	433,488 (100)
20GC	10,758,946	10,621,466	137,480 (1.3)	74,159 (54)	63,321 (46)	58,476 (92)
20GU	14,069,013	13,672,463	396,550 (2.8)	137,554 (35)	258,996 (65)	255,885 (99)
21GC	12,401,494	12,317,266	84,228 (0.7)	33,917 (40)	50,311 (60)	38,008 (76)
21GU	5,415,770	5,339,327	76,443 (1.4)	23,885 (31)	52,558 (69)	44,161 (84)

[a]Percentage of total reads. [b]Percentage of mapped reads. [c]Percentage of perfectly matching reads that align to the shRNA/AgoshRNA sequence.

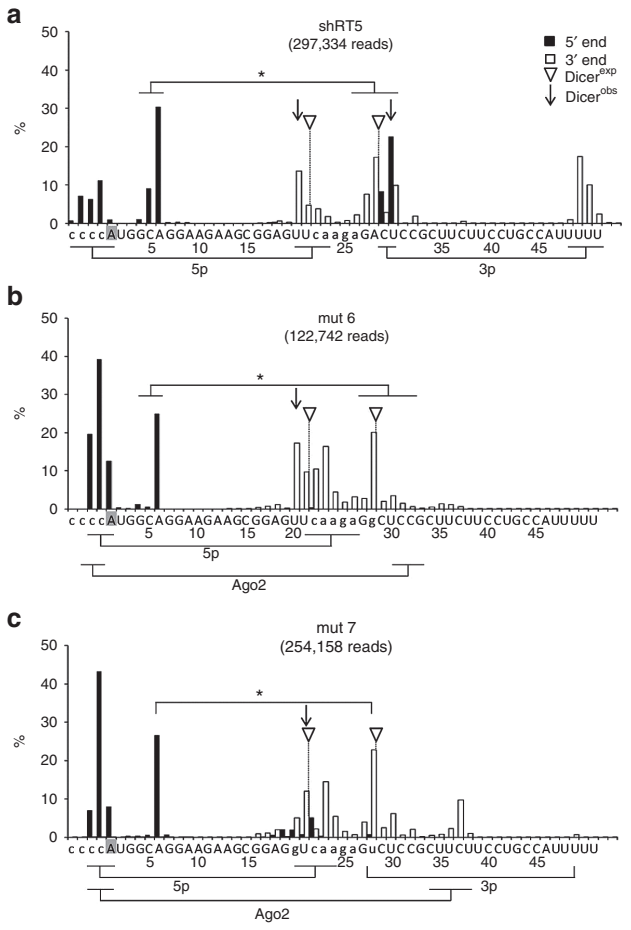

Figure 2 Sequence diversity of regular shRNA products. Deep sequencing analysis of the Ago2-bound RNAs for shRT5 (**a**), mut 6 (**b**), and mut7 (**c**) shows a variety of shRNA/AgoshRNA products. The cumulative incidence (y axis, depicted as % of total reads) of distinct 5' ends (black bars) and 3' ends (white bars) is shown along the shRNA sequence (x-axis, in capitals with the promoter and loop area in small letters). The total number of reads is indicated. Marked are the predicted transcription start site (boxed in gray), the predicted Dicer cleavage site (Dicer^{exp}; ◅) and the observed Dicer cleavage site (Dicer^{obs}; ←). The major cleavage products (Ago2, 5p, 3p and an extra fragment*) are indicated per graph.

Results

Deep sequence analysis of shRNAs with a G·U top base pair

We previously investigated whether replacement of a strong Watson-Crick bp by a weak G·U bp at the top of a shRNA stem could force the prototype 21 bp shRT5 hairpin (**Figure 1b**) into the AgoshRNA route.[28] This shRT5 was chosen as both 5p and 3p arms generated by Dicer are active in Luc-target silencing and it was shown to be the best inhibitor out of a set of AgoshRNAs.[29,35] Several mutations introduced in the top of the hairpin increased AgoshRNA activity, accompanied by appearance of the typical Ago2-cleaved product on northern blot.[28] RNA structures of shRT5 and mutants 6 and 7 and the previous results are summarized in **Figure 1b**. In short, mut 6 produced a modest AgoshRNA band on northern blot, but the regular Dicer cleavage products remained dominant. Mut 7 demonstrated a significant increase in Ago2-mediated processing and a concomitant decrease in Dicer cleavage. Gene silencing activity was measured with the Luc-sense reporter that scores the activity of the 3p strand and the Luc-antisense reporter for Dicer-cleaved 5p and the Ago2-cleaved AgoshRNA guide.[28,29] Reduced 3p strand activity was scored for mut 6 and 7, consistent with decreased Dicer cleavage.

We extracted Ago2-bound small RNAs to determine the relative amount of Dicer and Ago2 products by deep sequencing. Dominant reads (>50 copies in the library) are listed in **Supplementary Table S1**. For shRT5 and the two mutants, 96–99% of the plasmid-matching reads aligned to the expressed shRNA (**Table 1**). This high coverage permitted us to carefully map the content of the Ago2-bound RNAs. A major advantage of the AgoshRNA design over miRNA-like designs is that the Drosha-processing step is not needed to release the hairpin RNA, thus limiting the requirements for processing. Both the 5p and 3p Dicer products of shRT5 are equally present in Ago2 (**Figure 2a**). This confirms the symmetric nature of shRT5 and explains the silencing activity measured for both strands (**Figure 1b**; Luc). The reduced activity of the 3p strand compared to the 5p strand may reflect differential silencing activity of the two strands. A clear shift to 5p/AgoshRNA products was apparent for mutants 6 and 7 (**Figure 2b**,**c**). More Ago2-cleaved product was observed for mut 7 (9.7% of all reads) and mut 6 (1.3%) over the wild-type (wt) shRT5 (0.1%). This correlates with increased AgoshRNA production by mut 6 and especially mutant 7 on northern blot.[28] Surprisingly, the observed Ago2-cleaved product (←) was 2 nt shorter than the expected AgoshRNA product (◅) for wt and the two mutants (**Figure 1b**). Increased AgoshRNA loading coincided with decreased 3p-strand loading for both mutants but especially mutant 6, although 5p loading was maintained (**Figure 2b**,**c**). This 3p loading-deficiency correlates with the reported loss of 3p-mediated Luc silencing activity, although northern blotting did show normal 3p-strand production.[28]

Dicer cleavage is predicted to occur between U^{21} and C^{22} for 5p and between A^{28} and C^{29} for 3p (**Figure 1b**).[36,37] We carefully mapped the actual Dicer cleavage sites (**Figure 2a**). Dicer cleavage does not occur exactly at the predicted site (**Figure 2**), but rather at multiple sites around this position. In fact, the major Dicer-cleavage event creates a 2-nt staggered cut at U^{20} and U^{30}, whereas U^{21} and C^{29} were predicted (**Figure 2a**). The major Dicer products are thus 1 nt shorter than predicted. Overall, cleavage by Dicer is inaccurate and yields multiple products that are loaded in Ago2/RISC.

The product variation is further increased as the 5p transcripts display various 5' ends, likely reflecting differential start site usage by RNA polymerase III at the H1 promoter (**Figure 2**). In fact, only 1% of transcripts start at the predicted transcription start site for shRT5 (mut 6: 13% and mut 7: 9%), whereas 16% initiate at the -1 position for shRT5 (mut 6: 40% and mut 7: 49%). By inspection of the reads, we observed that the heterogeneity in Dicer cleavage site is not linked to this differential start site usage. Lastly, for all three constructs an additional read was observed that starts at A^{6} and terminates at A^{28} (**Figure 2**). We currently do not understand how this molecule is generated.

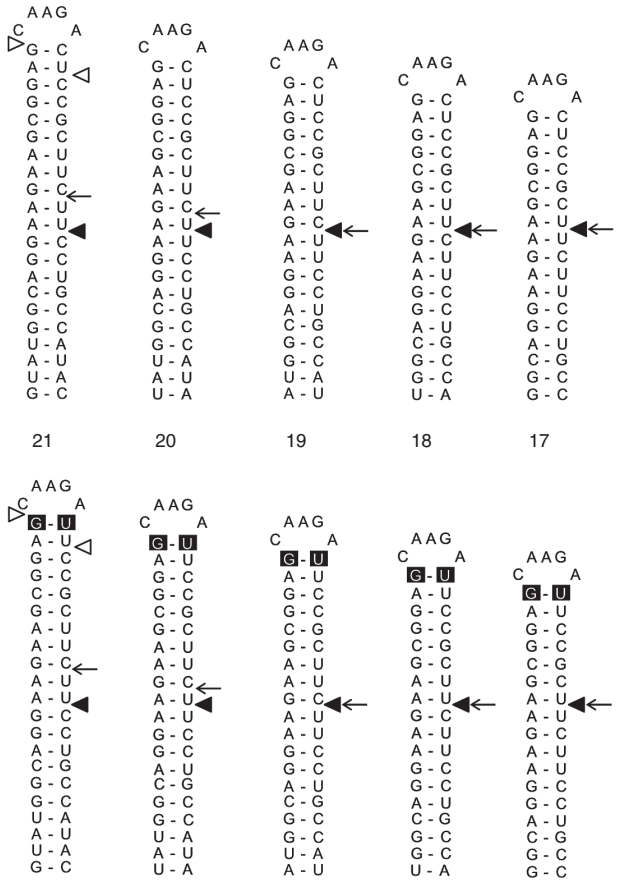

Figure 3 The shRT5 mutants with varying stem length. The 19/5 shRNA was elongated or shortened at the stem base to create a set of length mutants as described. The terminal top bp was mutated from G-C into a less stable G·U wobble bp (lower set, G·U wobble in a black box). Predicted Dicer (◅), predicted Ago2 (◄) and observed Ago2 (←) cleavage sites are indicated.

Deep sequence analysis of shRNAs/AgoshRNAs with varying stem length

Next, the shift from Dicer to Ago2 cleavage was analyzed for a second set of shRNAs with decreasing stem length and either a G·U or G-C top base pair. The expected cleavage products of Ago2 (◄) and Dicer (◅) are indicated on the hairpin templates in **Figure 3**. Some unexpected details of AgoshRNA processing were disclosed that will be discussed before we address the general shift from Dicer to Ago2 cleavage. As observed for mut 6 and 7, we witnessed a shift in the actual Ago2 cleavage site, and an intriguing pattern became apparent. For mutants 17/18/19, cleavage occurred exactly at the predicted position between bp 10–11 from the bottom of the stem, but cleavage shifted to bp 11–12 and 12–13 for mutants 20 and 21, respectively. The observed Ago2 cleavage sites are marked in **Figure 3** as arrows (←) and were used for quantitation of the AgoshRNA products. Inspection of the reads indicates that the transcripts with a shifted Ago2 cleavage site (mutants 20/21) do start at the same -1 position as mutants 17/18/19.

We observed a small 3' A-tail at the Ago2 cleavage site that is not encoded by the shRNA construct (**Table 2**). This tail is not due to sequencing errors as there are no adenines present around the Ago2 cleavage site. By use of ligation-based SOLiD deep sequencing, we also prevent any PCR-based errors that could have added A to the small RNA sequence. The A-tails are short with one to three adenines (**Table 3**) and the modified guide strand is named Agosh^{A}. No such 3' end modification was observed for Dicer-generated small RNAs. This 3' end modification was apparent for all wt and mutant shRNAs analyzed in this study, including the previously mentioned mut 7 (**Table 2**). Of all AgoshRNA guide strands, 27–87% contained a short 3' A-tail (**Table 2**). The Ago2-cleaved product was not prevalent for larger hairpins. No consistent pattern was apparent for 3' A-tailing with respect to stem length or GU/GC top.

Table 2 AgoshRNAs reads with 3' A addition

	No tail[a]	3' A(n)[a]	Total[a]	% no 3'[b]	% 3' A(n)[b]
17GC	897	1,514	2,411	37.2	62.8
17GU	23,534	22,328	45,862	51.3	48.7
18GC	303	2,090	2,393	12.7	87.3
18GU	496	337	833	59.5	40.5
19GC	754	3,126	3,880	19.4	80.6
19GU	972	3,736	4,708	20.6	79.4
20GC	403	553	956	42.2	57.8
20GU	335	126	461	72.7	27.3
shRT5	13	49	62	21.0	79.0
Mut 6	22	85	107	20.6	79.4
Mut 7	906	2,763	3,669	24.7	75.3

[a]number of reads. [b]Percentage of total number of AgoshRNA reads.

Table 3 Number of 3' As added to processed AgoshRNA molecules[a]

	17GC	17GU	18GC	18GU	19GC	19GU	20GC	20GU
A	95.9	94.3	93.7	90.8	94.7	99.6	70.3	88.1
AA	3.7	5.3	6.2	9.2	4.9	0.4	29.7	11.1
AAA	0.4	0.4	0.1	0.0	0.4	0.0	0.0	0.8

[a]Percentage of total number of AgoshRNA reads.

Inspired by recent findings for miR-451 and small nucleolar RNA (snoRNA), we reasoned that 3' adenylation may present a signal for PARN to trim the Agosh^{A} into the unpaired Agosh^{TRIM} molecule (**Figure 4a**).[38,39] Indeed, a distinct RNA population was observed that starts at the TSS and terminates just 3' of the shRNA loop (**Figure 4b**).

To determine the relative concentration of each RNA product, the shRNA-derived reads were defined as Dicer-cleaved (reads ranging from 19–22 nt, expected cleavage site ±1 nt), Ago2-cleaved Agosh^{A} (reads ≥27 nt, expected cleavage site ±1 nt) and Agosh^{TRIM} (reads between 23–28 nt and ending in the loop sequence AAGAc/uU (**Figure 4b**)). As expected, the regular 21 bp shRNA yields mostly Dicer-cleaved products ((**Figure 4c**,**d**) 55% for 21GC and 94% for 21GU; black line). The Dicer products disappear rapidly with decreasing shRNA stem length, concomitant with an increase of the Agosh^{A} and Agosh^{TRIM} products. The Agosh^{A} product remains a relatively minor product, never increasing above 4% of the total Ago2-bound RNA population (**Figure 4c**,**d**). Agosh^{TRIM} products constitute more than 50% of the RNA population for constructs with a small stem (≤ 19 bp), but are replaced by Dicer products for the larger hairpins (≥ 20 bp) (**Figure 4c**,**d**). No consistent differences were apparent for shRNAs with G-C or G·U as top bp.

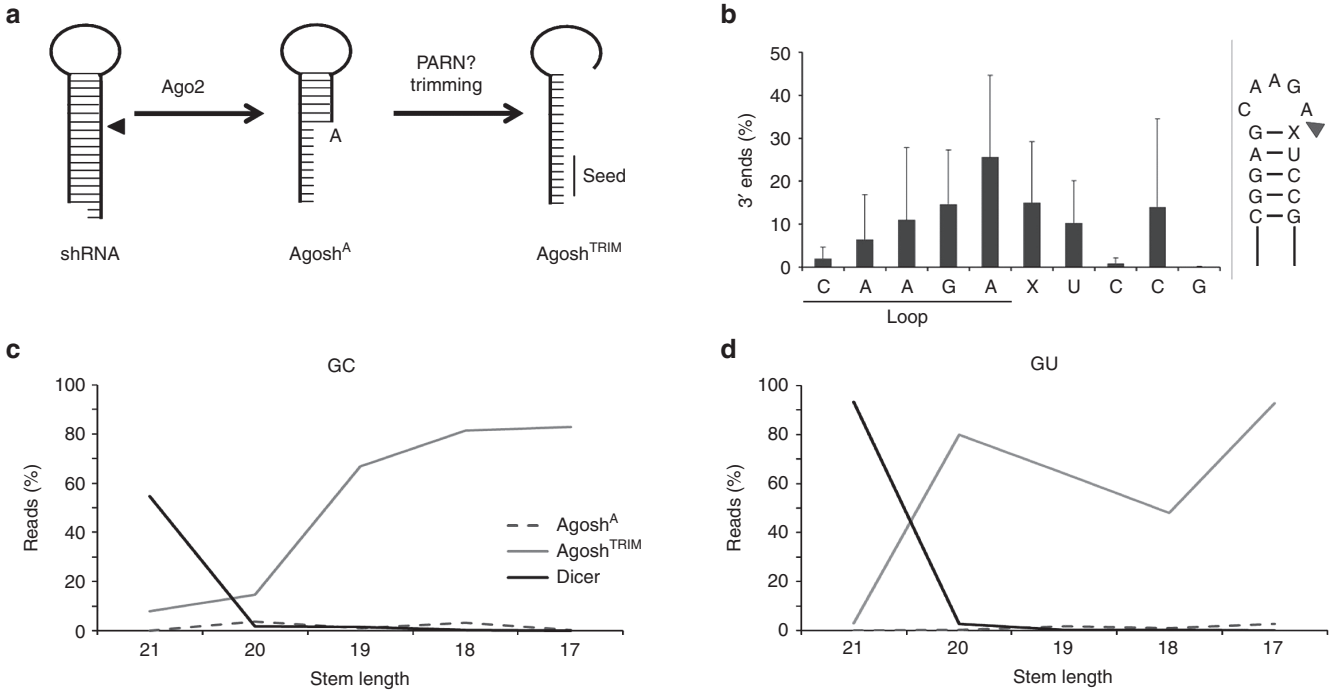

Figure 4 AgoshRNA processing and stem length. (**a**) Model for AgoshRNA processing. The AgoshRNA is cleaved by Ago2 into an Agosh guide and a small 3' A-tail is added to create Agosh^{A}, which is subsequently trimmed to Agosh^{TRIM}. (**b**) The 3' ends of the Agosh^{TRIM} population (incidence on y axis, depicted as % of total Agosh^{TRIM} reads) is shown along the AgoshRNA sequence (x-axis). X is C or U, depending on the mutant analyzed. On the left a small cartoon of the top AgoshRNA is shown with the major observed species after trimming (grey triangle). Average and standard variation was calculated for the complete shRNA/AgoshRNAs set. The major 3' end of Agosh^{TRIM} is marked as a gray triangle in the RNA structure cartoon. (**c**,**d**) The reads encoded by the GC set (panel **c**) and GU set (panel **d**) were used to calculate the incidence of Dicer (black line), Agosh^{A} (striped line), and Agosh^{TRIM} (gray line) products. Plotted is their percentage (y-axis, % of total reads) along the stem length (x-axis).

To further investigate the involvement of PARN in the generation of Agosh^{TRIM} products, we performed a PARN knockdown experiment with 18GC and 19GC. These constructs were chosen because they generate distinct AgoshRNA products.[28] The total RNA content of transfected cells was separated on a denaturing gel, blotted and probed with a locked nucleic acid probe directed against the 5' side of the hairpin (**Figure 5a**). This probe should thus detect Ago2 cleavage products as well as the Dicer-cleaved 5p strand. The knockdown of PARN caused the selective disappearance of the Agosh^{TRIM} product, while leaving the Dicer cleaved product intact (**Figure 5b**).

Discussion

Novel AgoshRNA designs form a promising class of RNAi-based therapeutics that avoid Dicer cleavage and instead use Ago2-slicer activity to create a single guide RNA to target a specific mRNA for destruction. AgoshRNAs thus avoid off-target effects induced by the passenger strand of a regular shRNA. We previously tested the critical elements, in particular the stem length, that cause a shift from regular shRNA to AgoshRNA activity.[28] The current deep sequencing analysis confirmed these findings by probing for Dicer versus Ago2 cleavage events. In addition, several novel details about AgoshRNA processing were disclosed.

Cleavage at the predicted site confirmed Ago2 cleavage for the shorter hairpins, but we noticed an upward shift in cleavage site for the less efficient AgoshRNAs larger than 19 bp for both mutant sets (**Figures 1b** and **3**). An intriguing pattern became apparent: cleavage of mutants 17/18/19 occurs exactly at the predicted position in the 3' arm between bp 10 and 11 from the bottom of the stem, but was shifted between bp 11–12 and 12–13 for mutants 20 and 21, respectively (**Figure 6a**). Mutants 19/20/21 support the new concept of "cleavage at 9 bp from the loop" instead of the well-established "10 bp from the bottom" rule. In search for a mechanistic explanation, it is important to realize that the extended hairpins are processed less efficiently by Ago2 (**Figure 4c**,**d**). We present a mechanistic model in which the 5' end of the AgoshRNA docks in the MID domain and the loop is near the PAZ domain (**Figure 6b**). We propose a structural realignment in the Ago2-containing complex because the extended hairpins sterically clash with the PAZ and/or MID domains that are in close contact with the hairpin. This structural Ago2 rearrangement may explain the loss of slicer activity. A similar steric problem was suggested to occur for Ago2-loaded hairpins with a large loop.[29] Structural rearrangement pushes the domains of Ago2 out of the optimal position, which can explain the cleavage to shift 1 or 2 bp further up in the stem, albeit at a greatly reduced efficiency. This mechanistic model also explains the unexpected PIWI cleavage sites observed for the initial mutant set with extended stems of 21 bp (**Figure 2**). Thus, the sequence of an AgoshRNA does not influence the actual cleavage site, which seems dictated primarily by the duplex length (and secondarily by the loop size, see Liu *et al.*[29]). Cleavage and subsequent trimming by PARN may

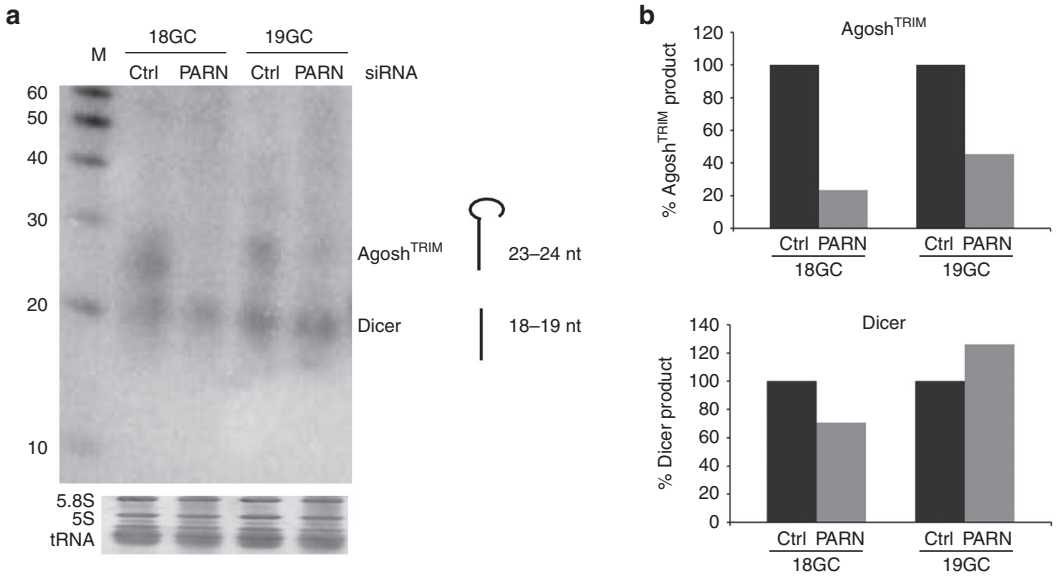

Figure 5 Knockdown of PARN. HEK-293T was transfected with 5 µg of the indicated AgoshRNA constructs and 50 nmol/l siRNA against PARN (PARN) and control (Ctrl). (**a**) Total RNA was isolated and analyzed by northern blot using an locked nucleic acid probe directed against the 5' side of the hairpin. The Agosh^{TRIM} and Dicer products are indicated. Size markers were included in the far left lanes and the length is indicated. Ethidium bromide staining of small rRNAs and tRNAs are shown as loading controls below the blot. (**b**) Quantification of Agosh^{TRIM} and Dicer products. The siCtrl-treated samples were set at 100%.

thus be essential to create a free 3' end that can dock into the PAZ domain to reach a stable configuration.[40–42] Single-stranded AgoshTRIM products will be accommodated in this stable Ago2 complex, thus blocking further PARN trimming and explaining the discrete trimming pattern (**Figure 4b**).

Another new finding is that a small 3' A-tail is added upon AgoshRNA cleavage to yield the modified Agosh^{A} guide strand (**Figure 4a**,**b**). We present evidence that this Agosh^{A} guide is a processing intermediate that is subsequently 3'-trimmed to generate a mature Agosh^{TRIM} RNA species (**Figure 4c**,**d**). The partially basepaired Agosh^{A} precursor becomes an unpaired Agosh^{TRIM}, thus activating its ability to pair with the mRNA to cause its inactivation. Further processing may be important as the RISC-Ago2 complex does not have RNA duplex unwinding activity.[43,44]

The PARN enzyme is the candidate for miR-451 trimming[39] and possibly AgoshRNA trimming. PARN also plays a role in deadenylation of maternal mRNAs during oocyte maturation,[45] mRNA degradation,[46] and maturation of mammalian box H/ACA small nucleolar RNAs.[38] PARN is a poly(A) specific exonuclease that uses 3' A-tails as substrate.[47] These short 3' A-tails could be added by poly(A) polymerases like PAPD5 (ref. [38]) or PAPD4 (ref. [8]), but details about what is recognized in AgoshRNAs and miR-451 remain unknown. We currently do not know if miR-451 is also 3' adenylated before it is trimmed by PARN. We specifically looked for such molecules, but miR-451 was absent from our 293T-based small RNA libraries. Upon knockdown of PARN, we witnessed a loss of the Agosh^{TRIM} product on northern blot (**Figure 5a**). This indicates that PARN is indeed involved in the generation of Agosh^{TRIM}. The regular Dicer product served as internal control that is not influenced by knockdown of PARN. PARN knockdown did not result in accumulation of the Agosh^{A} precursor, suggesting that it is an unstable intermediate.

Many RNAi applications use shRNA constructs to stably reduce gene expression, but it is becoming increasingly clear that these small RNA molecules are less precise than originally thought. This and other studies indicated that Dicer cleavage is rather imprecise, yielding multiple RNAs with different silencing efficiency, specificity and/or off-target effects.[48,49] Combined with the multiple transcriptional initiation sites observed for the H1 RNA polymerase in this and others studies, a quasispecies of slightly different guide RNAs is generated. The 5' end variation also holds for AgoshRNA reagents, but Ago2-mediated processing is more precise than Dicer cleavage. Another complicating factor is the choice of guide strand. Previous northern blot analysis indicated that mut 6 is processed into an equal concentration of 5p and 3p strands, however only the 5p strand showed activity (**Figure 1b**).[28] These northern blots were performed on total cellular RNA, but sequencing of the Ago2-bound RNA indicated that the 5p strand is exclusively loaded. This can explain the absence of 3p strand activity. To add to the small RNA diversity, we also describe an alternative transcript that runs from +6 to +28. We do not understand how this transcript is generated, whether it is alternatively processed or due to a new transcription initiation site. This aberrant RNA is loaded in Ago2 and therefore could theoretically cause gene silencing.

The generation of a single guide strand instead of two active shRNA-derived strands makes the AgoshRNA design an attractive reagent for biology applications and therapeutic action. This study and previous results indicate that an active AgoshRNA should have a stem-length of 19 bp and a small loop. The introduction of a top G·U wobble base pair can push a regular shRNA towards the AgoshRNA route, including subsequent tailing and trimming, as it likely reduces the stem length. However, a G·U top base pair does not influence processing of other AgoshRNAs. The AgoshRNA constructs

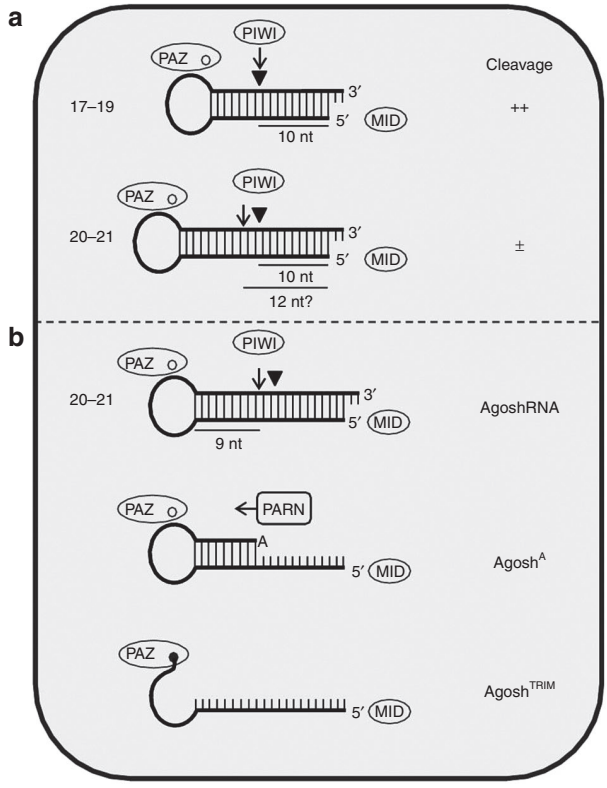

Figure 6 Models to explain aberrant cleavage of AgoshRNAs with an extended stem. (**a**) A regular AgoshRNA with a stem of 17–19 bp will dock into Ago2 with the 3' and 5' ends near the PAZ and MID domains, respectively. PIWI then cleaves the stem between bp 10–11. With increasing stem length (20–21 bp), AgoshRNA processing is profoundly reduced (right-hand column) and a remarkable shift in cleavage site occurs. (**b**) A model is proposed in which loading of the extended hairpin triggers rearrangement of Ago2 domains, causing the observed loss of cleavage efficiency and shift in cleavage site. Cleavage of the AgoshRNA yields the Agosh^{A}, which is subsequently trimmed by PARN into the Agosh^{TRIM} molecule. After trimming, the single-stranded 3' end of Agosh^{TRIM} can dock into the PAZ-domain to establish a stable Ago2-RNA complex.

may still be improved by approaches that yield a more precise transcript 5' end, either by changing the promoter or the transcription start site.

Materials and methods

Cell culture, transfection, and constructs. Human embryonic kidney (HEK-) 293T cells were cultured as monolayer in Dulbecco's modified Eagle's medium (Invitrogen, Paisley, UK) supplemented with 10% fetal bovine serum, penicillin (100 U/ml), and streptomycin (100 µg/ml) at 37 °C and 5% CO_2. For the RNA isolation, cells were cultured in 25 cm^2 flasks and transfected with 4 µg shRNA plasmid DNA and 1 µg Ago2-FLAG plasmid using lipofectamine 2000 (Life Technologies, Carlsbad, CA). The shRNA and AgoshRNA constructs used in this manuscript have been described previously.[28]

For PARN knockdown, HEK-293T were reverse transfected in 10 cm^2 wells with a siCtrl duplex[50] (5′-AAGCG AUACCUCGUGUGUGAdTdT-3′ and 5′-UCACACACGAGGU AUCGCUUdTdT-3′) and an siRNA mixture against PARN[39] consisting of siPARN duplex 1 (5′-GGAGAAAACAGGAAGAG AAdTdT-3′ and 5′-UUCUCUUCCUGUUUUCUCCdTdT-3′) and siPARN duplex 2 (5′-UCAUCUCCAUGGCCAAUUAdT dT-3′ and 5′-UAAUUGGCCAUGGAGAUGAdTdT-3′) using Lipofectamine 2000 (Life Technologies). After 48 hours, the siPARN-treated cells were reverse transfected with another 50 nmol/l of siRNA mixture and 5 µg of AgoshRNA-expressing construct. RNA was isolated 48 hours after the second transfection.

Ago2 immunoprecipitation, RNA isolation, and library preparation. At 48 hours post-transfection, the cells were washed several times with cold phosphate-buffered saline and Ago2-FLAG was immunoprecipitated as previously described.[29] In short, the cells were incubated with IsoB-NP40 (10 mmol/l Tris-HCl pH 7.9, 150 mmol/l NaCl, 1.5 mmol/l $MgCl_2$, 1% NP40) for 20 minutes on ice. The cell-lysates were centrifuged at 12,000 × g for 10 minutes at 4 °C to clear cell debris. The supernatant was incubated with 75 µl anti-FLAG M2 Agarose bead-suspension (Sigma, St Louis, MO) with constant rotation for 16 hours at 4 °C. The supernatant (depleted fraction) was separated from the beads (enriched fraction). The beads were washed three times with NET-1 buffer (50 mmol/l Tris-HCl pH 7.5, 150 mmol/l NaCl, 2.5% Tween-20) and resuspended in IsoB-NP40. RNA was isolated by phenol–chloroform extraction followed by DNAse treatment using the TURBO DNA-free kit (Life technologies). The isolated RNA was size separated on a 15% denaturing polyacrylamide gel electrophoresis gel next to a size marker (generuler ultra low range DNA ladder; Thermo Scientific, Waltham, MA) for size estimation. The 15–55 nt RNA fragments were purified from gel using a spin column (Ambion, Carlsbad, CA). The quality and percentage of miRNA was assayed on a Bioanalyzer 2100 (Agilent, Santa Clara, CA) using a small RNA chip. The SOLiD Small RNA Library Preparation protocol (Applied Biosystems, Carlsbad, CA) was used to prepare an RNA library that was subsequently analyzed on the SOLiD Wildfire system (Applied Biosystems).

Bioinformatics. Analysis of the SOLiD colorspace reads was performed with LifeScope Genomic Analysis Software version 2.5 (Applied Biosystems) using the small RNA pipeline. Analysis of the SOLiD deep sequence run yielded 6,796,533 to 14,069,013 reads per sample, with an average of 10,227,999 (**Table 1**). The libraries were cleaned for human genome filter sequences (containing rRNA, tRNA etc; supplied with LifeScope) and known miRNA sequences (miRBase version 21; http://www.mirbase.org/). Subsequently, the filtered reads were aligned against the reference sequences of the shRNA-expressing constructs. We performed two alignments to create read libraries; one containing perfect reads without mismatch, the other with a perfect seed region (nt 1–15) but with mismatches in the 3' part. For the different constructs, the combined libraries mapped 0.7–32.4%, with an average of 7.3% of all sequence reads to the reference sequence (**Table 1**). Of the mapping reads, 46–72% contained no mismatch (**Table 1**). This library without mismatch was used to create the final alignments and to analyze the Dicer and Ago2 cleavage products (shRNA and AgoshRNA, respectively). The library with 3' end mismatches was used to analyze nontemplated 3' end nt addition.

Supplementary material

Table S1. Abundant plasmid-encoded reads ($n > 50$) identified by SOLiD deep sequencing.

Acknowledgments. We thank Ted Bradley for help in SOLiD deep sequencing. This research was sponsored by the Netherlands Organization for Scientific Research (Chemical Sciences Division; NWO-CW; Top grant) and ZonMw (Translational Gene Therapy program).

1. Bartel, DP (2004). MicroRNAs: genomics, biogenesis, mechanism, and function. *Cell* **116**: 281–297.
2. Ha, M and Kim, VN (2014). Regulation of microRNA biogenesis. *Nat Rev Mol Cell Biol* **15**: 509–524.
3. Lee, Y, Ahn, C, Han, J, Choi, H, Kim, J, Yim, J *et al.* (2003). The nuclear RNase III Drosha initiates microRNA processing. *Nature* **425**: 415–419.
4. Shiohama, A, Sasaki, T, Noda, S, Minoshima, S and Shimizu, N (2003). Molecular cloning and expression analysis of a novel gene DGCR8 located in the DiGeorge syndrome chromosomal region. *Biochem Biophys Res Commun* **304**: 184–190.
5. Liu, YP and Berkhout, B (2013). Design of lentivirally expressed siRNAs. *Methods Mol Biol* **942**: 233–257.
6. Provost, P, Dishart, D, Doucet, J, Frendewey, D, Samuelsson, B and Rådmark, O (2002). Ribonuclease activity and RNA binding of recombinant human Dicer. *EMBO J* **21**: 5864–5874.
7. Zhang, H, Kolb, FA, Brondani, V, Billy, E and Filipowicz, W (2002). Human Dicer preferentially cleaves dsRNAs at their termini without a requirement for ATP. *EMBO J* **21**: 5875–5885.
8. Burroughs, AM, Ando, Y, de Hoon, MJ, Tomaru, Y, Nishibu, T, Ukekawa, R *et al.* (2010). A comprehensive survey of 3' animal miRNA modification events and a possible role for 3' adenylation in modulating miRNA targeting effectiveness. *Genome Res* **20**: 1398–1410.
9. Ebhardt, HA, Tsang, HH, Dai, DC, Liu, Y, Bostan, B and Fahlman, RP (2009). Meta-analysis of small RNA-sequencing errors reveals ubiquitous post-transcriptional RNA modifications. *Nucleic Acids Res* **37**: 2461–2470.
10. Landgraf, P, Rusu, M, Sheridan, R, Sewer, A, Iovino, N, Aravin, A *et al.* (2007). A mammalian microRNA expression atlas based on small RNA library sequencing. *Cell* **129**: 1401–1414.
11. Lim, J, Ha, M, Chang, H, Kwon, SC, Simanshu, DK, Patel, DJ *et al.* (2014). Uridylation by TUT4 and TUT7 marks mRNA for degradation. *Cell* **159**: 1365–1376.
12. Ren, G, Xie, M, Zhang, S, Vinovskis, C, Chen, X and Yu, B (2014). Methylation protects microRNAs from an AGO1-associated activity that uridylates 5' RNA fragments generated by AGO1 cleavage. *Proc Natl Acad Sci USA* **111**: 6365–6370.
13. Shen, B and Goodman, HM (2004). Uridine addition after microRNA-directed cleavage. *Science* **306**: 997.
14. Heo, I, Ha, M, Lim, J, Yoon, MJ, Park, JE, Kwon, SC *et al.* (2012). Mono-uridylation of pre-microRNA as a key step in the biogenesis of group II let-7 microRNAs. *Cell* **151**: 521–532.
15. Katoh, T, Sakaguchi, Y, Miyauchi, K, Suzuki, T, Kashiwabara, S, Baba, T *et al.* (2009). Selective stabilization of mammalian microRNAs by 3' adenylation mediated by the cytoplasmic poly(A) polymerase GLD-2. *Genes Dev* **23**: 433–438.
16. Czech, B and Hannon, GJ (2011). Small RNA sorting: matchmaking for Argonautes. *Nat Rev Genet* **12**: 19–31.
17. Elbashir, SM, Lendeckel, W and Tuschl, T (2001). RNA interference is mediated by 21- and 22-nucleotide RNAs. *Genes Dev* **15**: 188–200.
18. Hammond, SM, Boettcher, S, Caudy, AA, Kobayashi, R and Hannon, GJ (2001). Argonaute2, a link between genetic and biochemical analyses of RNAi. *Science* **293**: 1146–1150.
19. Liu, J, Carmell, MA, Rivas, FV, Marsden, CG, Thomson, JM, Song, JJ *et al.* (2004). Argonaute2 is the catalytic engine of mammalian RNAi. *Science* **305**: 1437–1441.
20. Meister, G, Landthaler, M, Patkaniowska, A, Dorsett, Y, Teng, G and Tuschl, T (2004). Human Argonaute2 mediates RNA cleavage targeted by miRNAs and siRNAs. *Mol Cell* **15**: 185–197.
21. Martinez, J, Patkaniowska, A, Urlaub, H, Lührmann, R and Tuschl, T (2002). Single-stranded antisense siRNAs guide target RNA cleavage in RNAi. *Cell* **110**: 563–574.
22. Khvorova, A, Reynolds, A and Jayasena, SD (2003). Functional siRNAs and miRNAs exhibit strand bias. *Cell* **115**: 209–216.
23. Schwarz, DS, Hutvágner, G, Du, T, Xu, Z, Aronin, N and Zamore, PD (2003). Asymmetry in the assembly of the RNAi enzyme complex. *Cell* **115**: 199–208.
24. Mourelatos, Z, Dostie, J, Paushkin, S, Sharma, A, Charroux, B, Abel, L *et al.* (2002). miRNPs: a novel class of ribonucleoproteins containing numerous microRNAs. *Genes Dev* **16**: 720–728.
25. Yang, JS and Lai, EC (2011). Alternative miRNA biogenesis pathways and the interpretation of core miRNA pathway mutants. *Mol Cell* **43**: 892–903.
26. Cheloufi, S, Dos Santos, CO, Chong, MM and Hannon, GJ (2010). A dicer-independent miRNA biogenesis pathway that requires Ago catalysis. *Nature* **465**: 584–589.
27. Tam, OH, Aravin, AA, Stein, P, Girard, A, Murchison, EP, Cheloufi, S *et al.* (2008). Pseudogene-derived small interfering RNAs regulate gene expression in mouse oocytes. *Nature* **453**: 534–538.
28. Herrera-Carrillo, E, Harwig, A, Liu, YP and Berkhout, B (2014). Probing the shRNA characteristics that hinder Dicer recognition and consequently allow Ago-mediated processing and AgoshRNA activity. *RNA* **20**: 1410–1418.
29. Liu, YP, Schopman, NC and Berkhout, B (2013). Dicer-independent processing of short hairpin RNAs. *Nucleic Acids Res* **41**: 3723–3733.
30. Dallas, A, Ilves, H, Ge, Q, Kumar, P, Shorenstein, J, Kazakov, SA *et al.* (2012). Right- and left-loop short shRNAs have distinct and unusual mechanisms of gene silencing. *Nucleic Acids Res* **40**: 9255–9271.
31. Ge, Q, Ilves, H, Dallas, A, Kumar, P, Shorenstein, J, Kazakov, SA *et al.* (2010). Minimal-length short hairpin RNAs: the relationship of structure and RNAi activity. *RNA* **16**: 106–117.
32. Cifuentes, D, Xue, H, Taylor, DW, Patnode, H, Mishima, Y, Cheloufi, S *et al.* (2010). A novel miRNA processing pathway independent of Dicer requires Argonaute2 catalytic activity. *Science* **328**: 1694–1698.
33. Ma, H, Zhang, J and Wu, H (2014). Designing Ago2-specific siRNA/shRNA to Avoid Competition with Endogenous miRNAs. *Mol Ther Nucleic Acids* **3**: e176.
34. Metzker, ML (2010). Sequencing technologies - the next generation. *Nat Rev Genet* **11**: 31–46.
35. ter Brake, O, Konstantinova, P, Ceylan, M and Berkhout, B (2006). Silencing of HIV-1 with RNA interference: a multiple shRNA approach. *Mol Ther* **14**: 883–892.
36. Macrae, IJ, Zhou, K, Li, F, Repic, A, Brooks, AN, Cande, WZ *et al.* (2006). Structural basis for double-stranded RNA processing by Dicer. *Science* **311**: 195–198.
37. Zhang, H, Kolb, FA, Jaskiewicz, L, Westhof, E and Filipowicz, W (2004). Single processing center models for human Dicer and bacterial RNase III. *Cell* **118**: 57–68.
38. Berndt, H, Harnisch, C, Rammelt, C, Stöhr, N, Zirkel, A, Dohm, JC *et al.* (2012). Maturation of mammalian H/ACA box snoRNAs: PAPD5-dependent adenylation and PARN-dependent trimming. *RNA* **18**: 958–972.
39. Yoda, M, Cifuentes, D, Izumi, N, Sakaguchi, Y, Suzuki, T, Giraldez, AJ *et al.* (2013). Poly(A)-specific ribonuclease mediates 3'-end trimming of Argonaute2-cleaved precursor microRNAs. *Cell Rep* **5**: 715–726.
40. Elkayam, E, Kuhn, CD, Tocilj, A, Haase, AD, Greene, EM, Hannon, GJ *et al.* (2012). The structure of human argonaute-2 in complex with miR-20a. *Cell* **150**: 100–110.
41. Wang, Y, Juranek, S, Li, H, Sheng, G, Tuschl, T and Patel, DJ (2008). Structure of an argonaute silencing complex with a seed-containing guide DNA and target RNA duplex. *Nature* **456**: 921–926.
42. Wang, Y, Sheng, G, Juranek, S, Tuschl, T and Patel, DJ (2008). Structure of the guide-strand-containing argonaute silencing complex. *Nature* **456**: 209–213.
43. Schirle, NT and MacRae, IJ (2012). The crystal structure of human Argonaute2. *Science* **336**: 1037–1040.
44. Schirle, NT, Sheu-Gruttadauria, J and MacRae, IJ (2014). Structural basis for microRNA targeting. *Science* **346**: 608–613.
45. Körner, CG, Wormington, M, Muckenthaler, M, Schneider, S, Dehlin, E and Wahle, E (1998). The deadenylating nuclease (DAN) is involved in poly(A) tail removal during the meiotic maturation of Xenopus oocytes. *EMBO J* **17**: 5427–5437.
46. Cevher, MA, Zhang, X, Fernandez, S, Kim, S, Baquero, J, Nilsson, P *et al.* (2010). Nuclear deadenylation/polyadenylation factors regulate 3' processing in response to DNA damage. *EMBO J* **29**: 1674–1687.
47. Körner, CG and Wahle, E (1997). Poly(A) tail shortening by a mammalian poly(A)-specific 3'-exoribonuclease. *J Biol Chem* **272**: 10448–10456.
48. Denise, H, Moschos, SA, Sidders, B, Burden, F, Perkins, H, Carter, N *et al.* (2014). Deep Sequencing Insights in Therapeutic shRNA Processing and siRNA Target Cleavage Precision. *Mol Ther Nucleic Acids* **3**: e145.
49. Gu, S, Jin, L, Zhang, Y, Huang, Y, Zhang, F, Valdmanis, PN *et al.* (2012). The loop position of shRNAs and pre-miRNAs is critical for the accuracy of dicer processing in vivo. *Cell* **151**: 900–911.
50. Cazalla, D, Xie, M and Steitz, JA (2011). A primate herpesvirus uses the integrator complex to generate viral microRNAs. *Mol Cell* **43**: 982–992.

Supplementary Information accompanies this paper on the Molecular Therapy–Nucleic Acids website (http://www.nature.com/mtna)